

Distinct roles for $G\alpha$ and $G\beta\gamma$ in regulating spindle position and orientation in *Caenorhabditis elegans* embryos

Monica Gotta* and Julie Ahringer*

*Wellcome/CRC Institute, Tennis Court Road, Cambridge, CB2 1QR, UK
e-mail: jaa@mole.bio.cam.ac.uk

Correct placement and orientation of the mitotic spindle is essential for segregation of localized components and positioning of daughter cells. Although these processes are important in many cells, few factors that regulate spindle placement are known. Previous work has shown that GPB-1, the $G\beta$ subunit of a heterotrimeric G protein, is required for orientation of early cell division axes in *C. elegans* embryos. Here we show that GOA-1 (a $G\alpha_o$) and the related GPA-16 are the functionally redundant $G\alpha$ subunits and that GPC-2 is the relevant $G\gamma$ subunit that is required for spindle orientation in the early embryo. We show that $G\alpha$ and $G\beta\gamma$ are involved in controlling distinct microtubule-dependent processes. $G\beta\gamma$ is important in regulating migration of the centrosome around the nucleus and hence in orientating the mitotic spindle. $G\alpha$ is required for asymmetric spindle positioning in the one-celled embryo.

Asymmetric cell divisions are critically important in generating cellular diversity. Prerequisites for asymmetric divisions are both the polarized distribution of cytoplasmic components and the proper alignment of the mitotic spindle. In *C. elegans*, the pattern of early cell division is invariant. Both astral microtubules and actin have roles in proper spindle orientation^{1–3}. However, the means by which different patterns of cell division are established is not yet understood. One component known to be involved is GPB-1, the β -subunit of a heterotrimeric G protein. In a *gpb-1* mutant, cell-division axes are randomly orientated within the cell⁴.

Heterotrimeric G proteins are composed of three polypeptides — an alpha subunit ($G\alpha$) that binds to and hydrolyses GTP, and beta ($G\beta$) and gamma ($G\gamma$) subunits, which act as a single functional $G\beta\gamma$ dimer. G proteins are inactive in the heterotrimeric form, in which $G\alpha$ is bound to GDP. Upon activation, $G\alpha$ exchanges GDP for GTP, causing the heterotrimer to dissociate into $G\alpha$ and $G\beta\gamma$ subunits, both of which can activate target effectors. GTP hydrolysis promotes reassociation of $G\alpha$ with $G\beta\gamma$, thus inhibiting $G\beta\gamma$ activity (reviewed in ref. 5).

In wild-type embryos, centrosomes duplicate and then migrate apart from one another on the surface of the nucleus until they are diametrically opposed. In most cells, the mitotic spindle is then set up on this axis; the path of migration thus determines spindle orientation. In the P (germline) lineage, a nucleocentrosomal rotation then occurs that results in orientation along a different division axis².

Previous work has shown that centrosome positions are abnormal just before nuclear-envelope breakdown (NEBD) in *gpb-1* mutants⁴. To understand better the nature of this defect, we monitored the migration paths of centrosomes and subsequent orientation of mitotic spindles when *gpb-1* activity was reduced by RNA interference (RNAi)⁶. In this approach, injection of double-stranded RNA corresponding to a gene of interest into a hermaphrodite specifically inhibits the expression of that gene in its progeny. The

phenotype obtained can approximate that of a null or reduction-of-function mutant. In *gpb-1(RNAi)* (hereafter referred to as *G β (RNAi)*) embryos, GPB-1 was not detectable (data not shown).

In *G β (RNAi)* embryos, spindle orientations are incorrect for several reasons — centrosomes migrate onto abnormal axes, rotation of the nucleocentrosomal complex in P1 cells is absent or late (the spindle, rather than the nucleocentrosomal complex, rotates), and/or ectopic rotation of the nucleocentrosomal complex occurs in cells in which such rotation should not occur (see Supplementary Information, Table S1). For example, in the daughters of the AB cell, ABa and ABp, although centrosomes always migrated in opposite directions from one another, they migrated onto a random axis, whereas in the wild type they always migrated onto the left/right axis. Furthermore, in many ABa cells, rotation of the nucleocentrosomal complex was observed after migration; this never occurred in wild-type ABa cells (Fig. 1b, e, g and Supplementary Information, Table S1). Therefore, GPB-1 is required for timely rotation of the nucleocentrosomal complex in P1 cells and for correct centrosome migration.

To identify the relevant $G\gamma$ subunit, we used RNAi to investigate the functions of the two *C. elegans* $G\gamma$ genes, *gpc-1* and *gpc-2* (ref. 7). *gpc-1(RNAi)* animals were 100% viable ($n = 200$), indicating that *gpc-1* is not required for embryonic development. Consistent with this observation, defects in *gpc-1* deletion mutants are confined to sensory neurones (G. Jansen and R. Plasterk, personal communication). However, 75% ($n = 311$) of *gpc-2(RNAi)* embryos (hereafter referred to as *G γ (RNAi)*) died. *G γ (RNAi)* embryos exhibit defects in spindle orientation that are identical to those in *gpb-1* mutants⁴ and *G β (RNAi)* embryos (Fig. 1b, c and data not shown), as would be expected for the $G\gamma$ partner. Furthermore, as in *gpb-1* mutants, embryonic polarity in *G γ (RNAi)* embryos was normal — the first cleavage of embryos was asymmetric, cell-cycle times in AB and P1 cells were normal and P granules were correctly segregated to the P lineage (data not shown). *gpc-1* and *gpc-2* do not seem to be functionally redundant, as simultaneous application of RNAi to *gpc-1* and *gpc-2* did not increase the penetrance of the spindle-orientation defects (data not shown). The partial lethality of *gpc-2(RNAi)* may be due to incomplete silencing by RNAi. These data show that GPC-2 is the $G\gamma$ partner of GPB-1 ($G\beta$) in controlling spindle orientation.

We next sought to identify the relevant $G\alpha$ subunit(s). *C. elegans* has 20 $G\alpha$ genes⁷, with one clear homologue of each of the four vertebrate $G\alpha$ classes — $G\alpha_{12}$ (*gpa-12*; ref. 7) $G\alpha_q$ (*egl-30*; ref. 8) $G\alpha_{i/o}$ (*goa-1*; ref. 9) and $G\alpha_s$ (*gsa-1*; ref. 10). The remaining 16 $G\alpha$ genes do not fall clearly into one of these classes. Deletion mutants exist for all 20 genes, and none seems to be required for spindle orientation, indicating that there may be some functional redundancy⁷. Fourteen $G\alpha$ genes are expressed almost exclusively in a small subset of chemosensory neurones⁷, making them unlikely candidates to function in spindle orientation in the early embryo. We investigated

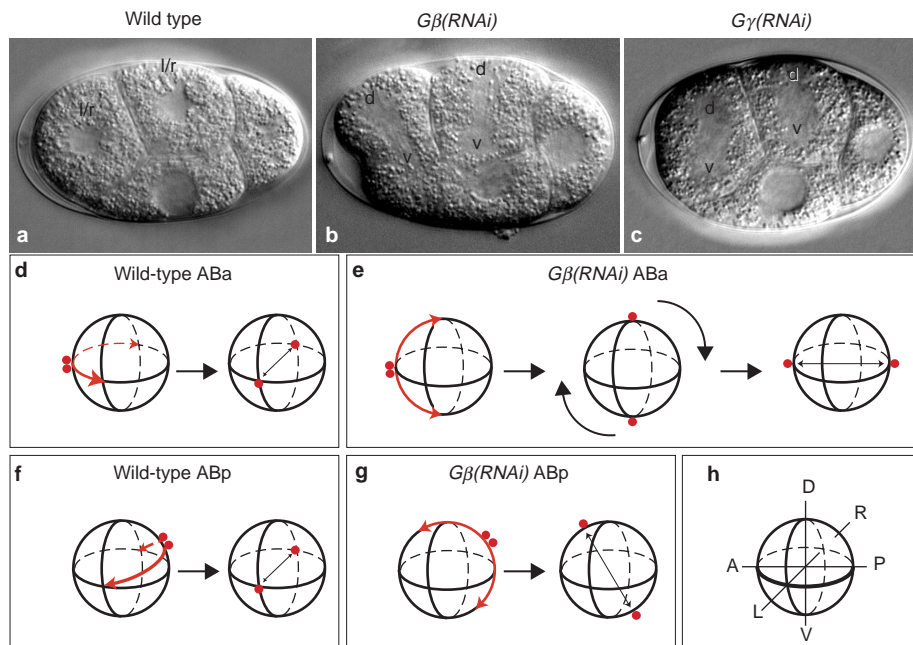


Figure 1 Spindle-orientation defects in *gpb-1(RNAi)* and *gpc-2(RNAi)* embryos. **a–c**, Wild-type **(a)**, *gpb-1(RNAi)* (*Gβ(RNAi)*) **(b)** and *gpc-2(RNAi)* (*Gγ(RNAi)*) **(c)** four-cell embryos. ABA and ABp cells are dividing (l/r, left/right; d, dorsal; v, ventral). In the wild type, spindles are orientated along the left/right axis (perpendicular to the plane of the image). In the *gpb-1(RNAi)* and *gpc-2(RNAi)* embryos shown, ABA and ABp spindles are orientated along the dorsal/ventral axis (the clear area between d and v). Other orientations also occur (see Supplementary

Information, Table S1). **d–g**, Centrosome movements in ABA **(d, e)** and ABp **(f, g)** cells in wild type **(d, f)** and *gpb-1(RNAi)* **(e, g)** embryos. Spheres represent nuclei, red dots represent centrosomes, and red arrows show paths of centrosome migration. Double-headed arrows represent the orientation of the spindle at division. Centrosome movements shown are representative of those in 17 embryos (see Supplementary Information, Table 1). **h**, Positions of the anteroposterior, dorsal/ventral and left/right axes of the spheres in **d–g**.

whether any of the remaining six genes (*goa-1*, *gsa-1*, *egl-30*, *gpa-12*, *gpa-7* and *gpa-16*), which are more widely expressed, are functionally redundant, using RNAi in pools (see Methods). Simultaneous inactivation of two of them, *goa-1* and *gpa-16*, resulted in 100% embryonic lethality ($n = 260$). Consistent with this redundancy in function, GPA-16 is the most similar $G\alpha$ to GOA-1 (63% identity with GOA-1 compared with 57% for the next closest $G\alpha$, GPA-7). We hereafter refer to *goa-1(RNAi)*; *gpa-16(RNAi)* embryos as *Gα(RNAi)* embryos.

Gα(RNAi) embryos exhibited several defects during early cleavages, the most striking of which was in centrosome separation from the two-cell stage onward. In 100% of wild-type embryonic cells, centrosomes were diametrically opposed before NEBD, and in P1 cells rotation had occurred (Fig. 2j and Supplementary Information, Table S1). In *Gα(RNAi)* embryos, centrosomes duplicated normally, as shown by the centrosome marker ZYG-9 (ref. 11; data not shown). However, centrosomes were opposed in only 4.5% of cells in *Gα(RNAi)* embryos before NEBD, and in 45.5% of cells centrosomes were separated by $<60^\circ$ (Fig. 2j). In addition, no nucleocentrosomal rotation occurred in P1 cells (see Supplementary Information, Table S1). At NEBD, adjacent centrosomes separated as the mitotic spindle was set up, along the axis specified by their positions just before NEBD (see Supplementary Information, Table S1). This axis was transverse to the anterior/posterior axis in the majority of AB and P1 cells, as in the wild type. In some cases, the starting positions of centrosomes in AB and P1 cells were incorrect, being lateral rather than at the pole; in these cells centrosomes separated and the mitotic spindle was set up along the a/p axis (see Supplementary Information, Table S1). In many ABA and ABp cells centrosomes migrated onto an axis other than the left/right (wild-type) axis, resulting in abnormal division axes (see Supplementary Information, Table S1). In summary, in *Gα(RNAi)*

embryos, centrosomes fail to separate properly before NEBD. Incorrect spindle orientations are the result of lack of rotation (in P1 cells), abnormal centrosome starting positions, or incorrect paths of centrosome migration.

Gα(RNAi) embryos also have other defects. First, the mitotic spindle fails to rock as it elongates, and the posterior aster is round rather than disc-shaped (Fig. 2d, e). Second, the first mitotic spindle is centrally located, resulting in an equal first cleavage, rather than being asymmetrically displaced towards the posterior (Fig. 2e, j). Third, after the first cleavage, nuclei are mispositioned, often remaining associated with the cortex instead of migrating to the centre of the cells (Fig. 2f). Fourth, cells sometimes contain multiple nuclei (data not shown, see Methods).

To confirm the RNAi results, we investigated whether *goa-1* and *gpa-16* mutants genetically interact. Embryos from mothers homozygous for *goa-1(n363)* are viable and those from *gpa-16(pk481)* homozygotes are 30% lethal; both have weak spindle-orientation defects (data not shown.) However, *goa-1 gpa-16/goa-1 +* mothers lay only dead embryos (100%, $n = 358$). These embryos exhibited most of the defects described above for double-RNAi embryos (data not shown). These data indicate that GOA-1 and GPA-16 are redundant $G\alpha$ partners of GPB-1.

Inactivating $G\alpha$ would lead both to loss of $G\alpha$ signalling and to constitutive activation of $G\beta\gamma$, as $G\beta\gamma$ is inactivated by interaction with $G\alpha^5$. To determine which of these effects causes the defects observed in *Gα(RNAi)* embryos, we compared the phenotype of loss of $G\alpha$ to that of loss of both $G\alpha$ and $G\beta$. The *Gα(RNAi)* centrosome-separation defect was significantly rescued by removal of *gpb-1* (that is, in *goa-1(RNAi)*; *gpa-16(RNAi)*; *gpb-1(RNAi)* triple-RNAi embryos, hereafter referred to as *Gα(RNAi)*; *Gβ(RNAi)*; Fig. 2j). This indicates that the failure to separate centrosomes is due to overactivity of $G\beta\gamma$.

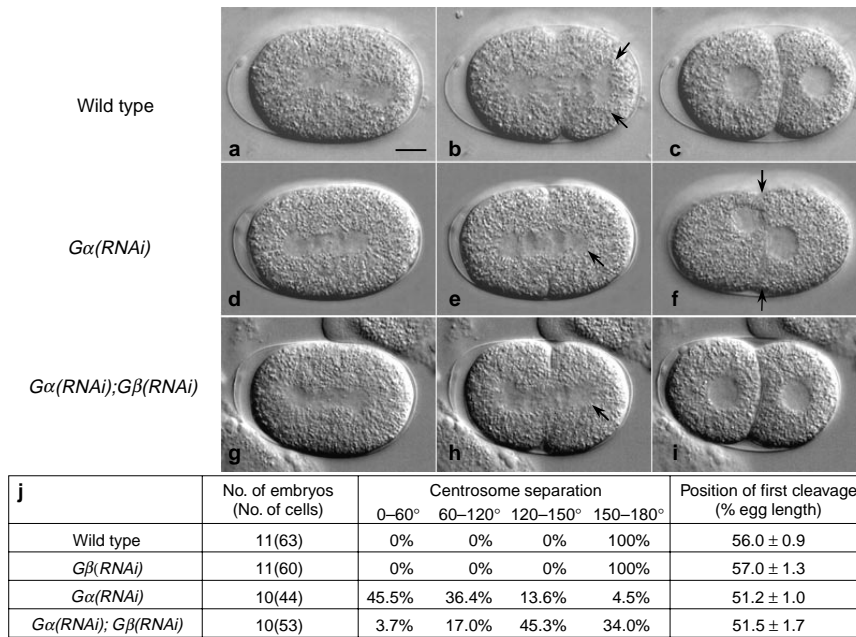


Figure 2 Heterotrimeric G proteins are required for a range of processes in the early embryo. Rocking of the mitotic spindle and a disc-shaped posterior aster are observed in wild-type (a, b), but not in *Gα(RNAi)* (d, e) or *Gα(RNAi); Gβ(RNAi)* (g, h) embryos. Arrows indicate the positions of asters. Spindle placement is asymmetric in wild-type embryos (b), but is symmetrical in *Gα(RNAi)* (e) and *Gα(RNAi); Gβ(RNAi)* (h) embryos. At the two-cell stage, nuclei are adjacent to the cortex in *Gα(RNAi)* embryos (f), but are central in wild-type (c) and *Gα(RNAi)*;

Gβ(RNAi) (i) embryos. Posterior is on the right in each case; scale bar represents 10 μm. In f the region of cell–cell contact (arrows) is not clearly visible because it is in a different plane of focus to nuclei. j, Degrees of centrosome separation (0° represents no separation; 150–180° represents full separation; see Methods) and the position of the first cleavage in wild-type and mutant embryos. Position of first cleavage is expressed as percentage of egg length (mean ± s.d.); anterior is designated as 0%.

We similarly examined the other defects observed in *Gα(RNAi)* embryos when *Gβ* was also inactivated. Like the centrosome-separation defect, the appearance of multiple nuclei per cell and abnormal cortical nuclear positioning defects seem to be due to constitutive activation of *Gβγ* (Fig. 2i and data not shown). However, in *Gα(RNAi); Gβ(RNAi)* embryos, the first cleavage was still symmetric, the posterior aster was round rather than flat, and no rocking occurred during spindle elongation (Fig. 2g–j). Although the mitotic spindle was symmetric in *Gα(RNAi)* embryos, polarity appeared to be normal, as PAR proteins were correctly localized and P granules segregated to the posterior (see Supplementary Information, Fig. S1). This indicates that *Gα* signalling is required in the one-cell embryo for proper behaviour and morphology of the mitotic spindle, including its asymmetric position in the cell, but is not required for embryonic polarity.

All of the defects in *Gα(RNAi)* embryos affect either the centrosomes and associated asters or the mitotic spindle, structures that are both composed of microtubules. We therefore tested whether the distribution of tubulin was affected. In 36 out of 36 wild-type embryos, asters were large and symmetrically organized (Fig. 3a, b). In contrast, in 23 out of 26 *Gα(RNAi)* embryos, tubulin distribution was disorganized, and asters were irregularly shaped in comparison to the wild type (Fig. 3c, d and Supplementary Information, Fig. S2). In 30 out of 35 *Gα(RNAi); Gβ(RNAi)* embryos, tubulin distribution was rescued, indicating that these defects are caused by constitutive activation of *Gβγ* (compare Fig. 3e, f with c, d). Both these phenotypes, failure of centrosome separation and abnormal tubulin distribution, are strikingly similar to the effects of taxol or nocodazole², indicating that hyperactive *Gβγ* may affect microtubule dynamics.

Previous work has shown that GPB-1 localizes at the cell membrane and on microtubule asters in wild-type embryos⁴. Using a

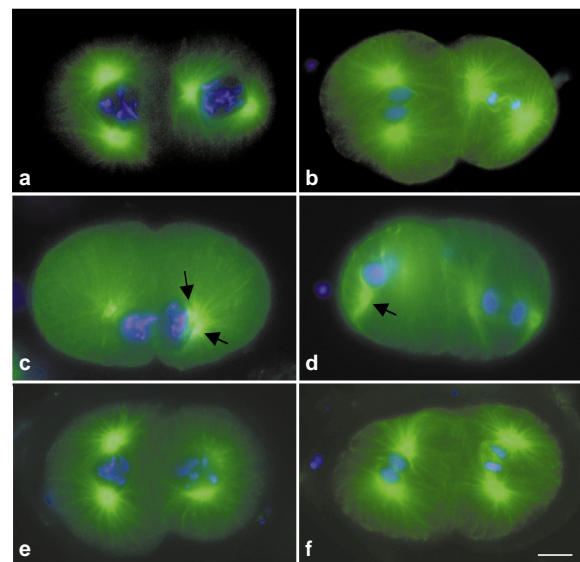


Figure 3 Tubulin distribution is abnormal in *Gα(RNAi)* embryos. Wild-type (a, b), *Gα(RNAi)* (c, d) and *Gα(RNAi); Gβ(RNAi)* (e, f) embryos stained for tubulin (green) and DNA (blue). a, c, e, Two-cell embryos in prophase. b, d, f, Two-cell embryos during division. Arsters appear to be well-organized in wild-type and *Gα(RNAi); Gβ(RNAi)* embryos compared with *Gα(RNAi)* embryos. Arrows in c show that centrosomes have duplicated but have not separated; this embryo is similar in age to those in a and e. Arrow in d shows an aster that is elongated, rather than round as in the wild type. *Gα(RNAi)* is *goa-1(RNAi)*; *gpa-16(RNAi)*. *Gα(RNAi); Gβ(RNAi)* is *goa-1(RNAi); gpa-16(RNAi)*; *gpb-1(RNAi)*. See Supplementary Information, Fig. S2. Posterior is to the right in each case; scale bar represents 10 μm.

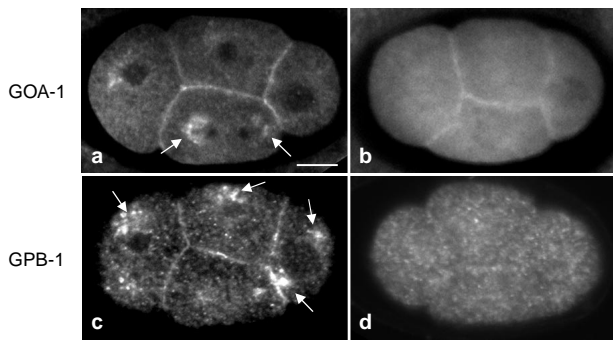


Figure 4 Immunolocalization of GOA-1 and GPB-1. GOA-1 localizes at the cell membrane and on asters in wild-type embryos (a), as does GPB-1 (c). This staining is specific, as it is absent from *goa-1* (*n363*) and *Gα(RNAi)* embryos (data not shown). In *Gβ(RNAi)* embryos, GOA-1 (b) localizes at the cell membrane but not on asters. GPB-1 (d) is both absent from asters and largely delocalized from the membrane in *Gα(RNAi)* embryos. *Gβ(RNAi)* is *gpb-1(RNAi)*. *Gα(RNAi)* is *goa-1(RNAi)*; *gpa-16(RNAi)*. In each case, at least 25 embryos were examined. Arrows indicate staining of the asters. Posterior is right in each case; scale bar represents 10 μm.

polyclonal antibody against GOA-1, we found that GOA-1 had the same localization pattern as that of GPB-1 (Fig. 4a, c). The localization of GOA-1 and GPB-1 to the same regions of the cell indicates that these may be sites of the heterotrimer. We also found that GOA-1 and GPB-1 were mutually dependent for their localization to asters (Fig. 4b, d). GPB-1 was also lost from the cell membrane in *Gα(RNAi)* embryos (Fig. 4d), although GOA-1 was still associated with the membrane in the absence of GPB-1 (Fig. 4b). The mutual dependence of the aster localization of GOA-1 and GPB-1 indicates that an intact heterotrimer may be required for movement to asters. Localization to asters, combined with the requirements for spindle and centrosome positioning, indicate that asters may be the normal site of activation and function of this heterotrimeric G protein.

Our data show that *Gα* is required for asymmetric placement and morphology of the mitotic spindle in the 1-cell embryo and that *Gβγ* is involved in regulating centrosome migration. The recent finding in *Drosophila* that a complex regulating spindle orientation contains Inscuteable, PINS and a *Gα_o* subunit¹² suggests that heterotrimeric G protein involvement in spindle orientation may be widespread.

We speculate that *Gβγ* may have both a positive and a negative role. It may participate in leading centrosomes to the correct place and at the same time inhibit all other possible routes around the nucleus. Perhaps, in the absence of *Gβγ*, centrosome migration is random because all routes around the nucleus are allowed. In contrast, when *Gβγ* is hyperactive (as in *Gα(RNAi)* embryos), centrosome migration is prevented because all routes are inhibited. When centrosomes partially separate in these embryos, they do so on the wrong axis, as is the case in *Gβ(RNAi)* embryos. Loss of *Gβγ* and constitutive *Gβγ* may therefore produce the same phenotype. Alternatively, this phenotype could be a result of lack of *Gα* signalling. One interesting feature is that nucleocentrosomal rotation in the P1 cell is often delayed in *gpb-1(RNAi)* and *gpb-1*-mutant embryos. Rotation depends on a connection between the aster and the cortex³, indicating that *Gβγ* may have a role in facilitating this connection. This in turn would indicate that *Gβγ* may control centrosome-migration axes through regulating interaction between asters and the cortex. Further studies, as well as the identification of downstream effectors, will help to elucidate the mechanisms by which *Gα* and *Gβγ* control positioning of the mitotic spindle. □

Methods

Strains and genetic methods.

The Bristol strain N2 was used as the standard wild-type strain. To confirm genetically the function of *goa-1* and *gpa-16* in controlling spindle orientation, the *goa-1*(*n363*) null allele⁹ and the *gpa-16*(*pk481*) allele⁷ were used.

Immunofluorescence.

Antibody staining was carried out as described¹³ with the following modifications: slides were blocked in PBS, 0.2% Tween and 1% milk, and all primary and secondary antibodies were diluted in PBS-Tween before use. The following primary antibodies were used: rabbit anti-GPB-1 (ref. 4); mouse anti-P-granule monoclonal cell supernatant (OIC1D4; ref. 14); rat monoclonal antibody YL1/2 against tubulin¹⁵; rabbit anti-PAR-2 (ref. 16); chicken anti-PAR-3 (ref. 17). The rabbit anti-GOA-1 antibody was raised against full-length GOA-1 and was a gift from M. Koelle (Yale Univ.).

RNA interference.

Templates for RNA synthesis were produced by polymerase chain reaction (PCR). For *gpb-1*, T3 and T7 primers were used on yk64c5 complementary DNA (provided by Yuji Kohara, Natl Inst. Genet., Japan). The open reading frames of *Gα* subunits were amplified from full-length cDNAs (provided by E. Cuppen and R. Plasterk, Hubrecht Lab.). For *gpc-1* and *gpc-2*, cDNAs were obtained by PCR with reverse transcription (RT-PCR) using the following primers: *gpc-1*, 5'-CGGGATCCGAATGGAAACATCAAGGCATCAAC and 5'-CCCAAGCTTTAGAGTACT-GAACAGCTTTTCTTC; *gpc-2*, 5'-CGGGATCCGAATGGATAAATCTGACATGCAACG and 5'-CCCAAGCTTTAGAGTACTGCTGCACTTGC. The cDNAs were cloned into the *Bam*H1 and *Hind*III sites of pBSKS- (Stratagene) and the plasmid was used as a template for PCR with T3 and T7 oligonucleotides. Sense and antisense RNAs for each gene were produced using RNA synthesis kits from Promega (ribomax) or Ambion (megascript) and were annealed before use. dsRNA was injected at a concentration of 0.5–1.0 mg ml⁻¹. To identify the relevant *Gα* subunits, dsRNA corresponding to six candidates (see text) were injected in two random pools of four (*gpa-16*, *gpa-1*, *goa-1* and *egl-30*, and *gpa-7*, *gpa-12*, *gpa-16* and *gpa-1*). The first pool gave 100% embryonic lethality, whereas the second produced only viable embryos. dsRNAs in the first pool were injected in all sets of two and individually. Only the combination of dsRNAs encoding *goa-1* and *gpa-16* caused 100% embryonic lethality.

Differential interference contrast 4D video microscopy.

Embryos from injected mothers were analysed 24–48 h after injection. Animals were dissected in a drop of M9 buffer on poly-L-lysine-coated coverslips (18 mm × 18 mm), mounted over an agar pad and sealed with vaseline. Embryos were recorded from the 1-cell to the 8-cell stage (15 focal planes every 30 s) with differential interference contrast optics on a Leica DMRBE microscope using Openlab software. Centrosome positions were assayed independently by two researchers in blastomeres at the 2-cell and 4-cell stages from 4D video recordings. Centrosomes were monitored from the birth of cells until their subsequent divisions. Angles of centrosome separation were measured from centrosome positions just before NEBD and were determined relative to the centre of the nucleus. The timing of NEBD in cells of *Gα(RNAi)* embryos was the same as that in wild-type cells (data not shown). Cells in which both centrosomes could not be identified were not included. Cells in which two nuclei were present in *Gα(RNAi)* embryos were also excluded; such cells represented <5% of cells at the 2-cell and 4-cell stages.

RECEIVED 18 APRIL 2000; REVISED 28 SEPTEMBER 2000; ACCEPTED 19 OCTOBER 2000; PUBLISHED 15 FEBRUARY 2001.

- Hill, D. P. & Strome, S. *Development* **108**, 159–172 (1990).
- Hyman, A. A. & White, J. G. *J. Cell Biol.* **105**, 2123–2135 (1987).
- Hyman, A. A. *J. Cell Biol.* **109**, 1185–1193 (1989).
- Zwaal, R. R. *et al. Cell* **86**, 619–629 (1996).
- Neer, E. *J. Cell* **80**, 249–257 (1995).
- Fire, A. *et al. Nature* **391**, 806–811 (1998).
- Jansen, G. *et al. Nature Genet* **21**, 414–419 (1999).
- Brundage, L. *et al. Neuron* **16**, 999–1009 (1996).
- Segalat, L., Elkes, D. A. & Kaplan, J. M. *Science* **267**, 1648–1651 (1995).
- Park, J. H., Ohshima, S., Tani, T. & Ohshima, Y. *Gene* **194**, 183–190 (1997).
- Matthews, L. R., Carter, P., Thierry-Mieg, D. & Kempthues, K. *J. Cell Biol.* **141**, 1159–1168 (1998).
- Schaefer, M., Shevchenko, A., Shevchenko, A. & Knoblich, J. A. *Curr. Biol.* **10**, 353–362 (2000).
- Guo, S. & Kempthues, K. *J. Cell* **81**, 611–620 (1995).
- Strome, S. & Wood, W. B. *Cell* **35**, 15–25 (1983).
- Kilmartin, J. V., Wright, B. & Milstein, C. *J. Cell Biol.* **93**, 576–582 (1982).
- Boyd, L., Guo, S., Levitan, D., Stinchcomb, D. T. & Kempthues, K. *J. Development* **122**, 3075–3084 (1996).
- Tabuse, Y. *et al. Development* **125**, 3607–3614 (1998).

ACKNOWLEDGEMENTS

We thank M. Koelle, J. Kilmartin, K. Kempthues and S. Strome for antibodies, Y. Kohara for cDNAs, and E. Cuppen, G. Jansen and R. Plasterk for plasmids, strains and suggestions. Some strains used in this study were from the *Caenorhabditis* Genetics Centre, which is supported by the NIH National Center for Research Resources (NCRR). We also thank A. H. Brand, A. G. Fraser, R. Kamath, M. Martinez-Campos, J. W. Raff, and M. Sohrmann for comments on the manuscript. This work was supported by a Wellcome Senior Research Fellowship (to J.A.), an HFSP long-term fellowship (to M.G.) and an EC TMR network grant.

Correspondence and requests for materials should be addressed to J.A. Supplementary Information is available on *Nature Cell Biology's* website (<http://cellbio.nature.com>) or as paper copy from the London editorial office of *Nature Cell Biology*.

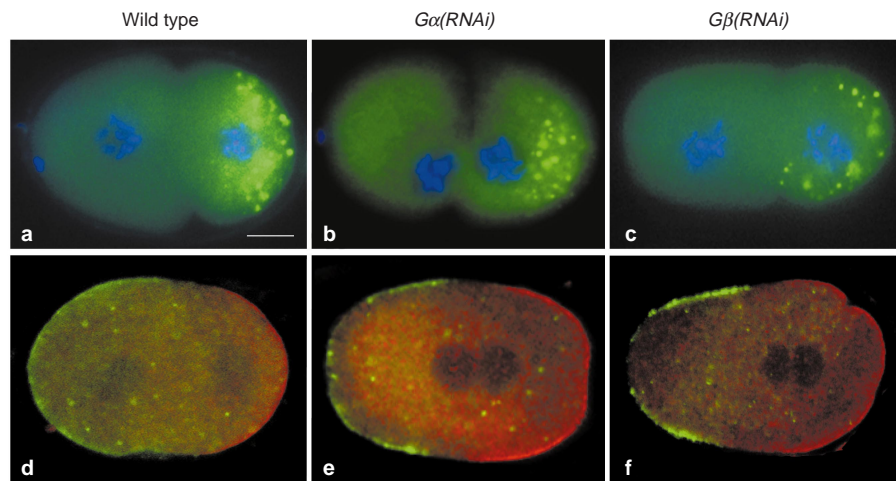


Figure S1 **Heterotrimeric G proteins are not required for embryonic polarity.** **a–c**, Localization of P granules (green) in wild-type (**a**), *Gα(RNAi)* (**b**) and *Gβ(RNAi)* (**c**) two-cell embryos. P granules are segregated to the posterior cell, P1, in both wild-type and mutant embryos. DNA is counterstained with DAPI (blue). **d–f**, Localization of PAR-2 (red) and PAR-3 (green) in wild-type (**d**), *Gα(RNAi)* (**e**) and

Gβ(RNAi) (**f**) one-cell embryos. In wild-type embryos PAR-3 and PAR-2 proteins are enriched at the anterior and posterior cortices, respectively. Localization of both PAR-3 and PAR-2 is normal in both *Gα(RNAi)* ($n = 25$), and *Gβ(RNAi)* ($n = 20$) embryos. Localization of PAR-2 and PAR-3 is also normal in two-cell embryos (data not shown). Posterior is to the right in each case; scale bar represents 10 μm .

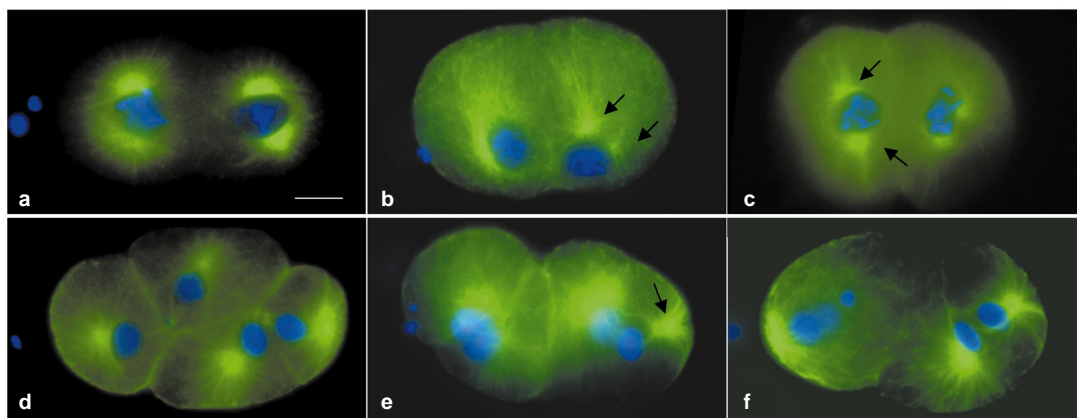


Figure S2 **Tubulin distribution is abnormal in *Gα(RNAi)* embryos.** Tubulin staining (green) in two-cell (**a–c**) and four-cell (**d–f**) embryos. **a, d**, Wild-type embryos; **b, c, e, f**, *Gα(RNAi)* embryos. This figure provides more examples for comparison of tubulin distribution and aster morphology in wild-type embryos and *Gα(RNAi)*

embryos. Arrows indicate centrosomes. DNA is counterstained with DAPI (blue). In **a** one aster of AB (the anterior cell) is out of focus. Posterior is to the right in each case; scale bar represents 10 μm .

Table S1 Centrosome migration paths and spindle orientations in wild-type, *Gβ(RNAi)* and *Gα(RNAi)* embryos.

	AB			P1			ABa			ABp		
	Migration	Rotation	Spindle orientation	Migration	Rotation	Spindle orientation	Migration	Rotation	Spindle orientation	Migration	Rotation	Spindle orientation
Wild type (n = 11)	Transverse	–	d/v	Transverse	+	a/p	l/r	–	l/r	l/r	–	l/r
<i>Gβ(RNAi)</i>	Transverse	–	d/v	Transverse	– *	a/p	ar/pl	+	l/r	d/v	–	d/v
<i>Gβ(RNAi)</i>	Transverse	–	d/v	Transverse	– *	a/p	d/v	+	a/p	dl/vr	–	dl/vr
<i>Gβ(RNAi)</i>	Transverse	–	d/v	Transverse	–	d/v	dr/vl	–	dr/vl	l/r	+	dr/vl
<i>Gβ(RNAi)</i>	Transverse	–	d/v	Transverse	– *	a/p	l/r	+	dr/vl	d/v	–	d/v
<i>Gβ(RNAi)</i>	Transverse	–	d/v	Transverse	+	a/p	dr/vl	–	dr/vl	d/v	–*	l/r
<i>Gβ(RNAi)</i>	Transverse	–	d/v	Transverse	+	a/p	l/r	+	a/p	dl/vr	–	dl/vr
<i>Gβ(RNAi)</i>	Transverse	–	d/v	Transverse	+	a/p	d/v	– *	dv/ap	dr/vl	–	dr/vl
<i>Gβ(RNAi)</i>	Transverse	–	d/v	Transverse	– *	a/p	l/r	+	a/p	dr/vl	–	dr/vl
<i>Gβ(RNAi)</i>	Transverse	–	d/v	Transverse	– *	a/p	l/r	+	a/p	al/pr	+	dr/vl
<i>Gβ(RNAi)</i>	Transverse	–	d/v	Transverse	– *	a/p	ns	ns	a/p	d/v	–	d/v
<i>Gβ(RNAi)</i>	Transverse	–	d/v	Transverse	– *	a/p	d/v	+	a/p	d/v	–	d/v
<i>Gβ(RNAi)</i>	Transverse	–	d/v	Transverse	– *	a/p	dl/vr	+	a/p	ar/pl	–	ar/pl
<i>Gβ(RNAi)</i>	Transverse	–	d/v	Transverse	+	a/p	ns	ns	al/pr	d/v	–	d/v
<i>Gβ(RNAi)</i>	Transverse	–	d/v	Transverse	+	a/p	l/r	+	a/p	dl/vr	–	dl/vr
<i>Gβ(RNAi)</i>	Transverse	–	d/v	Transverse	+	a/p	ns	ns	a/p	d/v	–	d/v
<i>Gβ(RNAi)</i>	Transverse	–	d/v	Transverse	–	d/v	dl/vr	–	dl/vr	d/v	–	d/v
<i>Gβ(RNAi)</i>	Transverse	–	d/v	Transverse	–	d/v	dr/vl	+	dr/vl	dl/vr	–	dl/vr
<i>Gα(RNAi)</i>	Transverse	–	d/v	Transverse	–	d/v	d/v	–	d/v	d/v	–	d/v
<i>Gα(RNAi)</i>	a/p†	–	a/p	a/p †	–	a/p	d/v ‡	–	d/v	d/v ‡	–	d/v
<i>Gα(RNAi)</i>	Transverse	–	d/v	a/p †	–	a/p	l/r ‡	–	l/r	dr/vl ‡	–	dr/vl
<i>Gα(RNAi)</i>	ns	ns	ns	Transverse	–	d/v	d/v	–	d/v	d/v	–	d/v
<i>Gα(RNAi)</i>	a/p†	–	a/p	Transverse	–	d/v	d/v	–	d/v	a/p †	–	a/p
<i>Gα(RNAi)</i>	Transverse	–	d/v	Transverse	–	d/v	dl/vr‡	–	dl/vr	dr/vl ‡	–	dr/vl
<i>Gα(RNAi)</i>	Transverse	–	d/v	a/p †	–	a/p	a/p †	–	a/p	a/p †	–	a/p
<i>Gα(RNAi)</i>	Transverse	–	d/v	Transverse	–	d/v	l/r	–	l/r	a/p †	–	a/p
<i>Gα(RNAi)</i>	Transverse	–	d/v	Transverse	–	d/v	ns	ns	ns	ns	ns	ns
<i>Gα(RNAi)</i>	a/p†	–	a/p	ns	ns	dv	d/v	–	d/v	a/p †	–	a/p

Table S1 **Centrosome migration paths and spindle orientations in wild-type, *Gβ(RNAi)* and *Gα(RNAi)* embryos.** Centrosome positions were monitored in wild-type and *gpb-1(RNAi)* AB, P1, ABa and ABp cells from birth until division, from 4D video recordings of embryonic development (15 focal planes per 30 s). ‘Migration’ indicates the axis defined by the migration path. As the d/v axis is not defined until the division of AB, wild-type migration in AB and P1 cells is designated as ‘transverse’, meaning transverse to the a/p axis. ‘Rotation’ indicates whether the nucleo-centrosomal complex rotated (+) or not (–); an asterisk indicates that the spindle

rotated. ‘Spindle orientation’ shows the final orientation of the mitotic spindle. In wild-type, *Gβ(RNAi)*, and *Gα(RNAi)* embryos, centrosomes migrate in opposite directions. The wild-type row shows data from 11 separate embryos. a, anterior; p, posterior; d, dorsal; v, ventral; l, left; r, right; ns, not scorable.

†Centrosome starting position was incorrect.

‡Centrosomes did not migrate apart from each other; this is probably the axis of centrosome duplication.